

Magnetohydrodynamic stability of negative central magnetic shear, high pressure ($\epsilon\beta_{pol}\gg 1$) toroidal equilibria

Robert G. Kleva

Institute for Plasma Research, University of Maryland, College Park, Maryland 20742-3511

(Received 24 June 1996; accepted 20 May 1997)

The magnetohydrodynamic (MHD) stability of negative central magnetic shear toroidal equilibria with $q > 2$ everywhere and $\epsilon\beta_{pol}\gg 1$ is investigated. Here, q is the safety factor of the equilibrium magnetic field in a torus with inverse aspect ratio ϵ , and β_{pol} is the ratio of the plasma pressure to the pressure in the poloidal magnetic field. At small $\epsilon\beta_{pol}\ll 1$, the elimination of the $q=2$ resonant surface in a negative shear equilibrium greatly improves resistive MHD stability as compared to equilibria with a monotonic q -profile containing a $q=2$ resonant surface. However, at large $\epsilon\beta_{pol}\gg 1$, the reversal of the central magnetic shear and the elimination of the $q=2$ resonant surface does not improve MHD stability. The existence, or non-existence, of rational magnetic surfaces has no impact on MHD stability when $\epsilon\beta_{pol}\gg 1$. Altering the current profile, and with it the q -profile, does not affect MHD stability when $\epsilon\beta_{pol}$ is no longer small. Stability is not improved by vertical elongation of the plasma in the poloidal plane. The utilization of an external vertical magnetic field to move the magnetic axis in major radius also does not improve MHD stability.
© 1997 American Institute of Physics. [S1070-664X(97)04108-6]

I. INTRODUCTION

High pressure tokamak equilibria with $\epsilon\beta_{pol}\gg 1$ are very different from low pressure equilibria with $\epsilon\beta_{pol}< 1$. Here, the poloidal beta β_{pol} is the ratio of the plasma pressure to the pressure in the poloidal magnetic field, and the inverse aspect ratio $\epsilon = a/R_0$ for a torus with major radius R_0 and minor radius a . In an $\epsilon\beta_{pol}\gg 1$ plasma bounded by a conducting wall, there is a large outward shift of the magnetic axis in major radius. The equilibrium flux function ψ is characterized by two asymptotic regions:¹ a core region on the small major radius side of the shifted magnetic axis in which ψ is solely a function of the major radial coordinate R , and a narrow boundary layer near the conducting wall.

In order for the tokamak to become an efficient, economic, and practical fusion reactor, operation at high β is very desirable. Therefore, the stability of these high $\epsilon\beta_{pol}$ equilibria is an important issue. Ideal ballooning modes have been found to be stable in large aspect ratio ($\epsilon \rightarrow 0$) toroidal equilibria with $\epsilon\beta_{pol}\gg 1$, but with the toroidal beta $\beta_{tor}\ll 1$.² In a previous paper³ I investigated the resistive magnetohydrodynamic (MHD) stability of high $\epsilon\beta_{pol}$ equilibria in a torus with a square conducting wall, including the effect of both the equilibrium current gradient and pressure gradient. These $\epsilon\beta_{pol}\gg 1$ equilibria had a monotonically increasing safety factor profile in which the safety factor at the magnetic axis q_0 was equal to unity. The principal results of this previous numerical study are as follows. (1) There is no "second stability regime" for MHD modes when $\epsilon\beta_{pol}\gg 1$. MHD modes become extremely unstable as $\epsilon\beta_{pol}$ becomes much larger than unity. (2) As the resistivity of the plasma decreases in large $\epsilon\beta_{pol}\gg 1$ equilibria, the growth rate of the mode remains large and is virtually independent of the magnitude of the resistivity. (3) A broad spectrum of toroidal mode numbers n is violently unstable at large $\epsilon\beta_{pol}\gg 1$, including modes with $n\gg 1$. (4) These

modes grow very rapidly, with a very short exponential growth time of the order of the Alfvén time.

Several recent tokamak experiments^{4,5} have demonstrated greatly improved particle and energy confinement when the magnetic shear s in the core of the discharge is reversed in sign. Here, the magnetic shear $s \equiv d(\ln q)/d(\ln r)$, where $q(r)$ is the safety factor profile in the minor radial coordinate r . Typically in these experiments, the safety factor profile q is peaked at the magnetic axis and decreases with distance from the magnetic axis until it reaches a minimum value q_{min} . The safety factor profile q then increases in a normal fashion towards the wall. Usually, the minimum value of q is larger than two so that the $q=2$ resonant surface is not in the plasma. A high β tokamak with the enhanced confinement produced by reversing the magnetic shear would make an attractive fusion reactor. Therefore, the effect of negative central magnetic shear on the MHD stability of high β equilibria is a matter of importance. MHD analyses of negative central magnetic shear equilibria have found that reversing the shear results in some improvement in marginal ideal MHD stability⁶⁻⁸ and a reduction in the growth of resistive tearing modes.⁷ However, the effect of negative magnetic shear on $\epsilon\beta_{pol}\gg 1$ equilibria has not been studied; the magnitude of the pressure used in prior analyses has not been large enough to access this regime. Thus, whether reversing the central magnetic shear improves MHD stability at large $\epsilon\beta_{pol}\gg 1$ has been unknown.

In this paper the resistive MHD stability of negative central magnetic shear, high $\epsilon\beta_{pol}\gg 1$ equilibria is studied in a torus with a conducting wall with a rectangular poloidal cross-section. The principal results of this numerical study are as follows. (1) The existence, or non-existence, of a rational magnetic surface has no impact on MHD stability when $\epsilon\beta_{pol}\gg 1$. Altering the current profile, and with it the q -profile, does not affect MHD stability when $\epsilon\beta_{pol}$ is no

longer small. (2) At low β_{pol} the removal of the $q=2$ surface from the plasma eliminates the growing $m=2/n=1$ resistive kink (tearing) mode, where m is the poloidal mode number, leaving a more weakly growing $m=3/n=1$ mode. However, as $\epsilon\beta_{pol}$ approaches unity, many MHD modes become unstable and the growth rate of these modes increases as $\epsilon\beta_{pol}$ becomes larger than unity. When $\epsilon\beta_{pol} \gg 1$, there is no significant difference in the MHD stability of negative shear equilibria without a $q=2$ surface and equilibria with monotonic q -profiles containing a $q=2$ surface. Both types of equilibria are violently unstable to a broad spectrum of rapidly growing MHD modes, including modes with $n \gg 1$, with a very short exponential growth time of the order of the Alfvén time. (3) The elongation of the poloidal cross-section in the vertical direction does not improve the MHD stability of $\epsilon\beta_{pol} \gg 1$ negative shear equilibria. (4) The utilization of an external vertical magnetic field to move the magnetic axis inward in major radius also does not improve the MHD stability of $\epsilon\beta_{pol} \gg 1$ negative shear equilibria.

The rest of this paper is organized as follows. An example of a high β , negative central magnetic shear tokamak equilibrium with $\epsilon\beta_{pol} \gg 1$ and $q > 2$ everywhere is presented in Sec. II. The MHD stability of these equilibria is discussed in Sec. III. The stability of negative shear equilibria without a $q=2$ resonant surface in the plasma is compared to that of equilibria with monotonically increasing q -profiles containing a $q=2$ resonant surface. The functional dependence of the growth rate on the magnitude of the plasma resistivity and on the toroidal mode number n of the perturbation is investigated. In Sec. IV the effect on stability of varying the poloidal cross-section from a square to a rectangle elongated in the vertical direction is considered. The utilization of an external vertical magnetic field to alter the equilibrium position of the magnetic axis is investigated in Sec. V. The results are discussed in Sec. VI.

II. NEGATIVE CENTRAL MAGNETIC SHEAR EQUILIBRIA

Axisymmetric negative central magnetic shear equilibria are obtained by solving the two-dimensional MHD equations dynamically. A discussion of the method of solution, and definitions of the normalized variables used in the MHD equations, is given in Ref. 3. The poloidal flux ψ is initially given by

$$\psi = Af(x/a_R)f(z/a_z), \quad (1)$$

where $x=R-R_0$ is the distance from the center of the plasma column along the major axis, a_R is the half-width of the rectangular cross-section in the direction of the major radius R , and a_z is the half-width of the rectangular cross-section in the vertical direction z . The function $f(y)$ is defined as

$$f(y) = \int_{-1}^y \left[1 + \kappa \frac{(u/b)^2}{1+(u/b)^4} \right] \frac{udu}{(1+\alpha u^{2\ell})^{1/\ell}}, \quad (2)$$

where $\alpha \equiv [(\bar{q}/q_0)^\ell - 1]$, \bar{q} , and ℓ are parameters³ and q_0 is the safety factor at the magnetic axis. The parameter A in Eq. (1) is given by $A \equiv a_R a_z R B_\phi / [R_0 q_0 f(0)]$. The parameters

κ and b in Eq. (2) determine the extent to which the magnetic shear is reversed near the magnetic axis; the magnitude of the reversal in the safety factor profile increases with κ while the distance from the magnetic axis over which the shear is reversed increases with b . The pressure is given by a flux function: $P = P_{max} g(\psi)/g(1)$, where $g(\psi) = \exp(\psi^b) - 1$, and the normalized flux $\psi = 1$ at the magnetic axis and $\psi = 0$ at the wall (separatrix). In all of the numerical results which follow, the major radius $R_0 = 3$ and the geometric minor half-width $a \equiv (a_R a_z)^{1/2} = 1$. Thus, the inverse aspect ratio $\epsilon \equiv a/R_0 = 1/3$. The safety factor profile is initially specified by $q_0 = 4.0$, $\bar{q} = 4.5$, $\ell = 4$, $\kappa = 2.0$, and $b = 0.4$. The mass density is uniform; $\rho = 1$. Let $\Delta\psi$ denote the total amount of poloidal magnetic flux in the equilibrium. The ratio of the plasma pressure to the pressure in the poloidal magnetic field is defined as $\beta_{pol} \equiv P_{max}/(\Delta\psi/aR_0)^2$. Equilibria with different β_{pol} are obtained by varying the maximum pressure P_{max} . The number of grid points retained in the simulations has been varied to ensure that the numerical results are insensitive to this number.

An example of a negative central magnetic shear, large $\epsilon\beta_{pol}$ equilibria obtained by dynamic relaxation is shown in Fig. 1. Figure 1(a) is a plot of contours of constant flux ψ in the (R, z) plane for an equilibrium plasma bounded by a square conducting wall with $\epsilon\beta_{pol} = 10.6$ ($\beta_{pol} = 31.8$). As the system settles into equilibrium, the magnetic axis, which was initially centered at $(R=R_0=3, z=0)$, shifts outward in major radius. A plot of constant pressure contours in this equilibrium is shown in Fig. 1(b). Profiles of the safety factor q (solid line) and the pressure (dashed line) through the mid-plane $z=0$ are shown in Fig. 1(c). The safety factor q approaches infinity at the bounding wall; the boundary is a magnetic separatrix, like the separatrix in a tokamak with a divertor. The safety factor profile is slightly jittery near the magnetic axis at $R=3.70$ (where $q_0=4.0$). The reason for this artificial numerical result is that flux surfaces near the magnetic axis encompass only a few grid points in the numerical simulation. As the magnetic field lines wander between grid points, a linear extrapolation of the magnitude of the magnetic field between grid points is used in calculating q . When the value of the safety factor changes rapidly with distance from the magnetic axis, as is the case for this reverse central shear equilibrium, then linear extrapolation is a poor approximation to the magnitude of the magnetic field. The minimum value of q is 2.2 in this equilibrium. Thus, the results in Fig. 1(c) demonstrate that the central magnetic shear is reversed in this $\epsilon\beta_{pol} = 10.6$ equilibrium, and that the safety factor q is larger than two everywhere. In the normalized units defined in Ref. 3, the total toroidal plasma current I_p is given by $I_p/aB_{\phi 0} = 0.18$, where $B_{\phi 0}$ is the magnitude of the vacuum toroidal magnetic field at the center $(x=0, z=0)$ of the column. The toroidal β , averaged over flux surfaces with $P(\psi) \geq 0.1P_{max}$, is $\langle \beta_{tor} \rangle = 10\%$. Note from Fig. 1(a) and Fig. 1(b) that both the flux and the pressure at the small major radius side of the magnetic axis are nearly independent of z , and are solely functions of the major radius R .

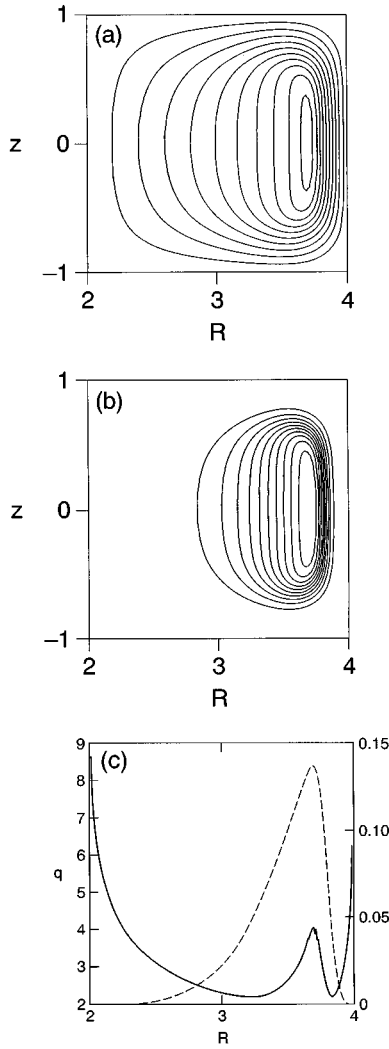


FIG. 1. Large $\epsilon\beta_{pol}$, negative central magnetic shear equilibrium. Contours of constant flux in an $\epsilon\beta_{pol}=10.6$ equilibrium in the poloidal (R, z) plane are plotted in (a), and constant pressure contours are plotted in (b). Profiles of the safety factor q (solid line) and the pressure P (dashed line) through the midplane ($z=0$) are plotted in (c).

III. NEGATIVE CENTRAL MAGNETIC SHEAR STABILITY

The MHD stability of two-dimensional toroidal equilibria with negative central magnetic shear to three-dimensional perturbations is obtained by solving the linearized MHD equations.³ The circles in Fig. 2 are a plot of the growth rate of a perturbation with toroidal mode number $n=1$ in negative shear equilibria characterized by a q -profile with q on axis $q_0=4.0$ and with a minimum value $q_{min}=2.2$, as a function of $\epsilon\beta_{pol}$, when $\eta=\mu=1\times 10^{-4}$. The bounding conducting wall is square ($a_R=a_z=1$). The equilibrium for $\epsilon\beta_{pol}=10.6$ is shown in Fig. 1. When $\epsilon\beta_{pol}\ll 1$, the growth rate, normalized to the Alfvén time $\tau_A\equiv a/V_A$ where V_A is the Alfvén velocity,³ is small. For a negative shear equilibrium with $q>2$ and $\epsilon\beta_{pol}=3.0\times 10^{-3}$, the growth rate is only 9×10^{-5} . However, as $\epsilon\beta_{pol}$ increases towards unity, the growth rate increases rapidly. When $\epsilon\beta_{pol}$ increases to 10.6, the growth rate rises to 6×10^{-2} ; the exponential growth time is only a little longer than ten Alfvén times.

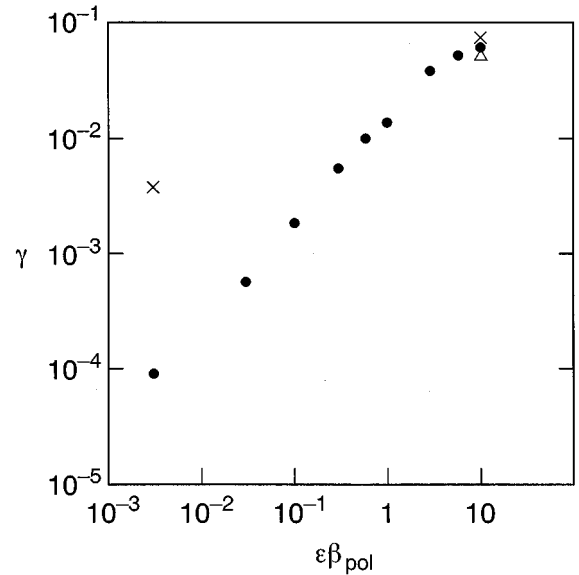


FIG. 2. MHD stability. The growth rate γ , normalized to the Alfvén time, is plotted as a function of $\epsilon\beta_{pol}$ on a log-log scale for equilibria with negative central magnetic shear and $q>2$ (circles), for equilibria with monotonically increasing q -profiles with $q_0=1.1$ (crosses), and for an equilibrium with an extended region of negative shear (open triangle).

For comparison, the MHD stability of equilibria with a monotonic q -profile is also shown in Fig. 2. The growth rate of an $n=1$ perturbation in equilibria where q increases monotonically away from the magnetic axis ($\kappa=0$) is given by the crosses in Fig. 2. The q -profile is flat (shearless) in the vicinity of the magnetic axis² and $q_0=1.1$. When $\epsilon\beta_{pol}=3.0\times 10^{-3}$ the growth rate is 4×10^{-3} , more than 40 times larger than it is in the reverse shear equilibrium with $q>2$ at the same value of $\epsilon\beta_{pol}$. Thus, the elimination of the $q=2$ resonant surface and the reversal of the central magnetic shear leads to a large reduction in the resistive MHD growth rate in low β equilibria with $\epsilon\beta_{pol}\ll 1$. However, when $\epsilon\beta_{pol}=10.6$, the growth rate of the $n=1$ mode in the equilibrium with a monotonic q -profile differs only slightly from that in the negative shear equilibrium. Therefore, the elimination of the $q=2$ resonant surface and the reversal of the central magnetic shear does not improve MHD stability at large $\epsilon\beta_{pol}\gg 1$.

The structure of the growing $n=1$ mode in the small $\epsilon\beta_{pol}=3.0\times 10^{-3}$ equilibrium is shown in Fig. 3. Level contours of the real part of the pressure perturbation in the poloidal plane are plotted in this figure. Figure 3(a) shows the structure of the $n=1$ mode in the negative shear equilibrium with $q>2$. At small $\epsilon\beta_{pol}$ the structure of the pressure is characterized by three maxima and three minima in the poloidal plane. If one defines a poloidal angle θ relative to the magnetic axis, measured from the midplane at $z=0$, then the variation of the pressure with θ is dominantly given by $\cos(m\theta)$ with $m=3$. Thus, the pressure at small $\epsilon\beta_{pol}$ has the characteristic $m=3/n=1$ structure of low β resistive kink (tearing) MHD modes which resonate with the equilibrium magnetic field at the $q=3$ resonant surface. For comparison, the structure of the $n=1$ mode in the equilibrium with a monotonic q -profile with $q_0=1.1$ is shown in Fig.

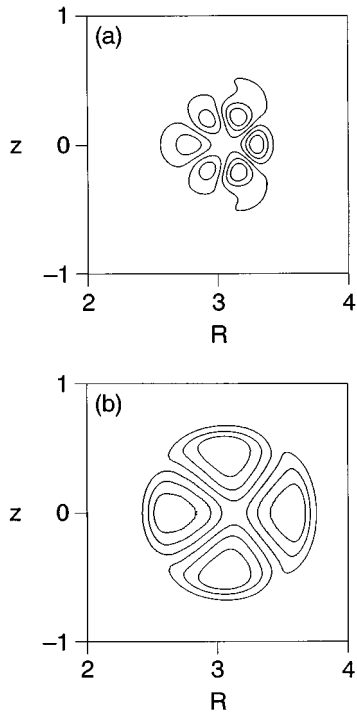


FIG. 3. Mode structure at small $\epsilon\beta_{pol}$. The real part of the pressure perturbation of the $n=1$ mode is plotted for an equilibrium with $\epsilon\beta_{pol}=3.0\times 10^{-3}$ and (a) negative central magnetic shear with $q>2$, and (b) a monotonic q -profile with $q_0=1.1$.

3(b). There are two maxima and two minima in the poloidal plane; the mode is an $m=2/n=1$ resistive kink (tearing) mode which resonates with the equilibrium magnetic field at the $q=2$ resonant surface. Reversing the central magnetic shear and raising q above two everywhere eliminates this weakly growing $m=2/n=1$ resistive mode, leaving an even more weakly growing $m=3/n=1$ resistive mode. As the plasma becomes hotter and the resistivity decreases, the growth rate becomes weaker yet.³

The physical picture is entirely different at large $\epsilon\beta_{pol}\gg 1$. The structure of the $n=1$ pressure perturbation when $\epsilon\beta_{pol}=10.6$ is shown in Fig. 4. Figure 4(a) is a plot of the real part of the pressure in the negative shear equilibrium with $q>2$, while a corresponding plot of the pressure perturbation in the equilibrium with a monotonic q -profile with $q_0=1.1$ is shown in Fig. 4(b). The structure of the mode in the two cases is similar. No evidence of the existence of the $q=2$ resonant surface in the plasma, or the lack thereof, can be seen. And the growth rate of the mode in these two equilibria is nearly the same.

Extending the region over which the magnetic shear is negative does not improve MHD stability at large $\epsilon\beta_{pol}$. Figure 5 is a plot of the q -profile (solid line) and the pressure profile (dashed line) for a negative shear equilibrium identical to that shown in Fig. 1, except that $b=0.75$ instead of 0.4; increasing b increases the distance from the magnetic axis over which the shear is negative. For the equilibrium shown in Fig. 5, virtually all of the plasma pressure is confined to the region of negative magnetic shear. The stability of an $n=1$ perturbation in this equilibrium is given by the triangular point in Fig. 2. There is only a small change in the

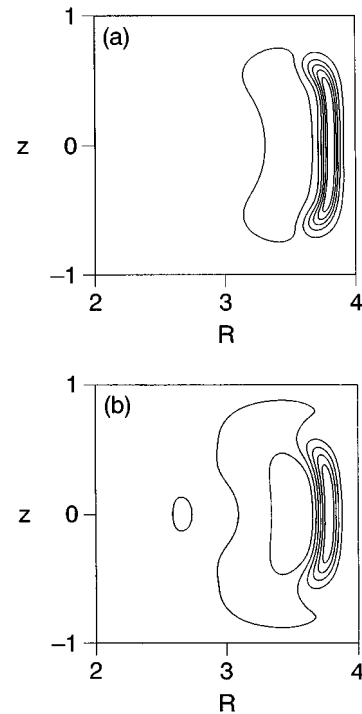


FIG. 4. Mode structure at large $\epsilon\beta_{pol}$. The real part of the pressure perturbation of the $n=1$ mode is plotted for an equilibrium with $\epsilon\beta_{pol}=10.6$ and (a) negative central magnetic shear with $q>2$, and (b) a monotonic q -profile with $q_0=1.1$.

growth rate when the region of negative shear is extended. The very small decrease in the growth rate is probably due to the fact that the magnetic axis is shifted a little further outward toward the wall, from $R_{axis}=3.70$ to $R_{axis}=3.73$. Since the equilibrium gradients are shifted a little closer to the wall, the stabilizing tendency of the wall becomes a little more effective, although nowhere near sufficient to over-

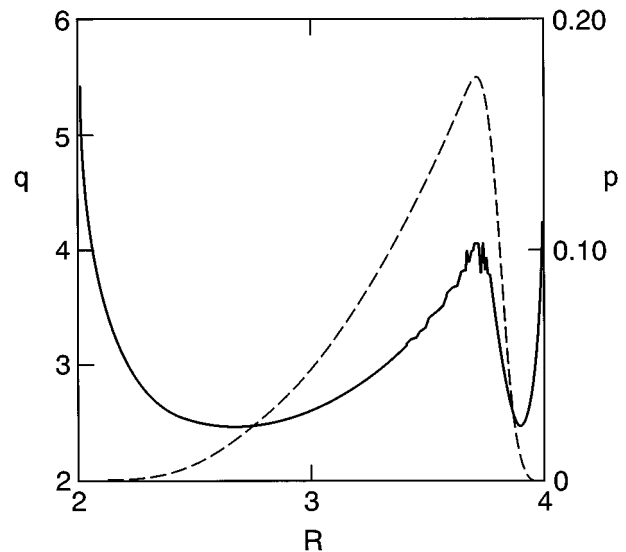


FIG. 5. Equilibrium with an extended region of negative shear. The safety factor profile q (solid line) and the pressure profile P (dashed line) through the midplane ($z=0$) are plotted.

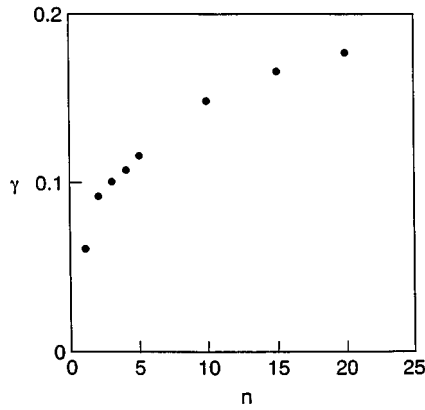


FIG. 6. Toroidal mode number. The growth rate γ , normalized to the Alfvén time, is plotted for perturbations with toroidal mode number n in a negative shear equilibrium with $\epsilon\beta_{pol}=10.6$.

come the large source of instability provided by the equilibrium gradients in the pressure and the current.

Magnetohydrodynamic stability at large $\epsilon\beta_{pol}$ is not improved by broadening the pressure profile. This has been checked by generating an equilibrium in which the pressure profile is flat at the magnetic axis; i.e., $dP/d\psi=0$. (For the more peaked equilibrium pressure profile shown in Fig. 1, $dP/d\psi\neq 0$ at the magnetic axis.) Flattening the pressure profile at the magnetic axis produces virtually no change in the growth rate of the $n=1$ mode at large $\epsilon\beta_{pol}$.

All of the stability results presented thus far have been for perturbations with toroidal mode number $n=1$. Figure 6 is a plot of the growth rate as a function of the toroidal mode number n of the perturbation, in the negative central magnetic shear equilibrium with $\epsilon\beta_{pol}=10.6$. As was found to be the case for $\epsilon\beta_{pol}\gg 1$ equilibria with a monotonic q -profile and with a $q=2$ resonant surface in the plasma,³ a broad spectrum of toroidal mode numbers is unstable and modes with $n>1$ grow even more rapidly than the $n=1$ mode. Thus, again we see that when $\epsilon\beta_{pol}\gg 1$, the removal of the $q=2$ surface from the plasma and/or the reversal of the central magnetic shear does not improve the MHD stability of the plasma.

The effect of the resistivity of the plasma on the growth rate of MHD modes in a high pressure ($\epsilon\beta_{pol}=10.6$), negative central magnetic shear equilibrium is shown in Fig. 7, where the growth rate of the $n=1$ (circles) and $n=10$ (crosses) modes is plotted as a function of the Lundquist number $S=\eta^{-1}$. The growth rate of the $n=1$ mode is virtually independent of the magnitude of the resistivity. The growth rate of the $n=10$ mode, which has shorter scale spatial structures than the $n=1$ mode, has an extremely weak dependence on S . Suppose that the scaling of the growth rate of the $n=10$ mode with S is given by a power law, $\gamma\sim S^{-\alpha}$. Then, fitting this power law to the two points with the largest values of S in Fig. 7, one finds that the exponent α is only 0.07.

There are two sources of free energy which can drive instabilities in MHD: the gradient in the pressure and the gradient in the parallel (to the magnetic field) current J_{\parallel} . In the ballooning approximation, the parallel current is ignored

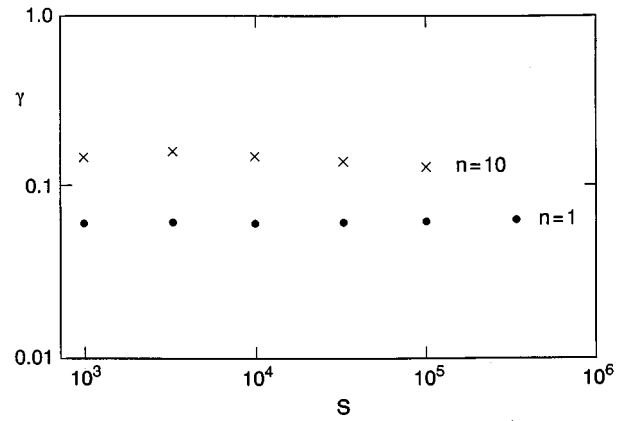


FIG. 7. Resistivity dependence of the growth rate. The growth rate γ , normalized to the Alfvén time, is plotted as a function of the Lundquist number $S=\eta^{-1}$ on a log-log scale for the $n=1$ mode (circles) and the $n=10$ mode (crosses) in a negative shear equilibrium with $\epsilon\beta_{pol}=10.6$.

and only the pressure is retained as a source of instability. If the parallel current in the $\epsilon\beta_{pol}=10.6$ equilibrium is neglected in the stability analysis of the large $n=20$ mode, then the growth rate of the mode decreases by 10%; the mode is dominantly driven by the equilibrium pressure gradient. Although there is a small decrease in the growth rate, the large $n=20$ mode remains unstable in the ballooning approximation. In contrast, the ideal ballooning mode was found to be stable in $\epsilon\beta_{pol}\gg 1$ equilibria in Ref. 2. However, in addition to the ballooning approximations $n\rightarrow\infty$ and $J_{\parallel}=0$, several other approximations are made in Ref. 2 to simplify the analysis, none of which are made in the simulations reported in this paper. Although $\beta_{pol}\rightarrow\infty$, only the $\beta_{tor}\ll 1$ limit is treated in Ref. 2. As a result, the poloidal curvature is neglected and the diamagnetic effect of the pressure on the toroidal magnetic field is also neglected. Furthermore, only the large aspect ratio $\epsilon\rightarrow 0$ limit is treated in Ref. 2, and effects of the order of $\epsilon^{1/2}$ are ignored. As a consequence, among other approximations, the normal curvature of the toroidal magnetic field on the large major radius side of the magnetic axis where the pressure gradient is the largest is neglected, in addition to the already neglected poloidal curvature. Both the resistivity and the compressibility of the plasma are also neglected in Ref. 2. None of the approximations in Ref. 2 are made in the simulations reported in this paper. The results in this paper are obtained by solving the fully compressible MHD equations, including the plasma resistivity. In the $\epsilon\beta_{pol}=10.6$ toroidal equilibrium, the large pressure digs a diamagnetic well in the toroidal magnetic field and the toroidal β on axis is $\beta_{tor}=30\%$. The inverse aspect ratio $\epsilon=1/3$ and $\epsilon^{1/2}\approx 0.6$, not a small number. And all components of the equilibrium current and the magnetic field, both toroidal and poloidal, are included in the calculations.

IV. POLOIDAL CROSS-SECTION

Consider now the effect on stability of altering the shape of the poloidal cross-section from a square to a rectangle elongated in the vertical direction. Suppose that the cross-

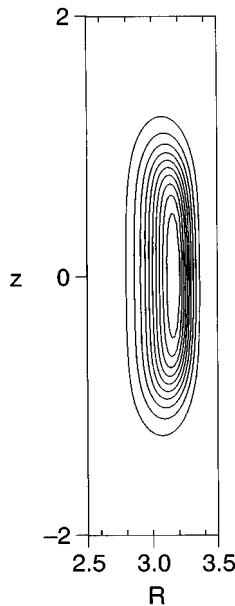


FIG. 8. Poloidal aspect ratio — equilibrium. Level contours of the pressure are plotted for a vertically elongated negative shear equilibrium with $\epsilon\beta_{pol}=10.6$ and poloidal aspect ratio $A_{pol}=4$.

sectional area $A=(2a_z)(2a_R)$ remains unchanged and equal to four as the shape of the poloidal cross-section is varied. Contour plots of the pressure for equilibria with two different values of the poloidal aspect ratio $A_{pol}\equiv a_z/a_R$ are shown in Figs. 1(b) and 8, for large $\epsilon\beta_{pol}=10.6$. As the cross-section is elongated vertically, the outward shift of the magnetic axis towards the wall becomes smaller. For a square plasma cross-section with $A_{pol}=1$, the magnetic axis is shifted outward 70% of the distance from the center of the column to the wall. For a vertically elongated cross-section with $A_{pol}=2$ the outward shift of the magnetic axis is reduced to 55%, while for a vertically elongated plasma cross-section with $A_{pol}=4$ the magnetic axis is shifted outward only 36% of the distance from the center of the column to the wall. Concomitantly, the gradient in the pressure on the large major radius side of the magnetic axis becomes shallower as the plasma is elongated vertically. As the cross-section is elongated, the magnitude of q on axis remains equal to 4.0 and the minimum value of q remains equal to 2.2.

The stability of MHD modes in the large $\epsilon\beta_{pol}=10.6$ equilibrium shown in Figs. 1 and 8 is presented in Fig. 9. This figure is a plot of the growth rate of the $n=1$ (circles) and $n=10$ (crosses) modes as a function of the poloidal aspect ratio. These results demonstrate that variation of the poloidal cross-section has virtually no impact on stability at large $\epsilon\beta_{pol}$. MHD modes remain violently unstable, with only a minor change in the magnitude of the growth rate, as the poloidal aspect ratio is changed. As the poloidal cross-section is elongated vertically, the equilibrium changes in two ways, with opposite consequences for stability. First, the equilibrium gradients on the large major radius side of the magnetic axis are somewhat reduced in magnitude, which reduces the source of the instability. At the same time the magnetic axis and the location of the equilibrium gradients are moved further away from the conducting wall, which

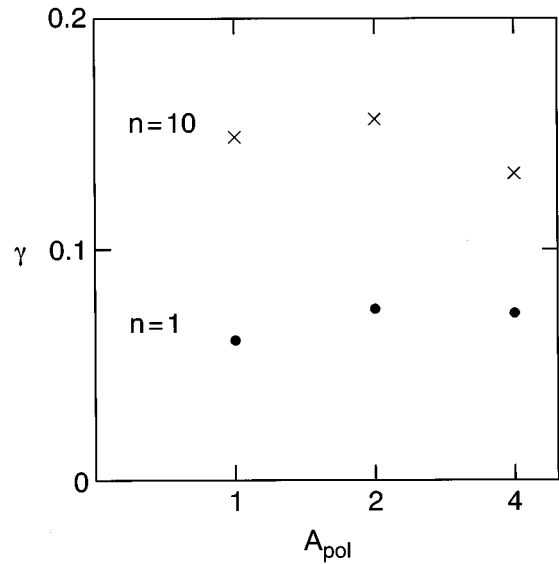


FIG. 9. Poloidal aspect ratio — stability. The growth rate γ , normalized to the Alfvén time, for the $n=1$ mode (circles) and the $n=10$ mode (crosses) is plotted as a function of the poloidal aspect ratio A_{pol} on a linear-log scale.

reduces the stabilizing influence of the wall. The net result is that variation of the poloidal aspect ratio has only a minor impact on stability. These results show that the cross-sectional shape of the wall does not have a strong effect on stability when $\epsilon\beta_{pol}\gg 1$; the stability is dominated by the steep gradients in the equilibrium pressure and current that are the sources of free energy.

The structure of the unstable $n=1$ mode in the poloidal plane is shown in Fig. 4(a) and Fig. 10. Level contours of the real part of the pressure perturbation are shown in these figures. When the plasma column is elongated vertically, the mode structure is rather diffuse and the mode extends over much of the equilibrium pressure profile. As the vertical

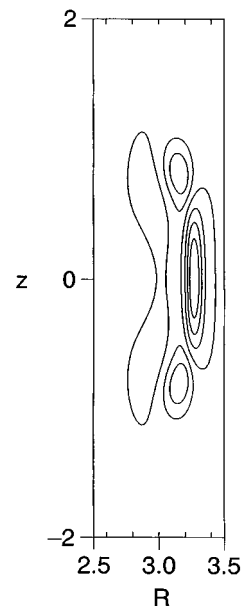


FIG. 10. Poloidal aspect ratio— $n=1$ mode structure. Level contours of the real part of the $n=1$ pressure perturbation are plotted for $A_{pol}=4$.

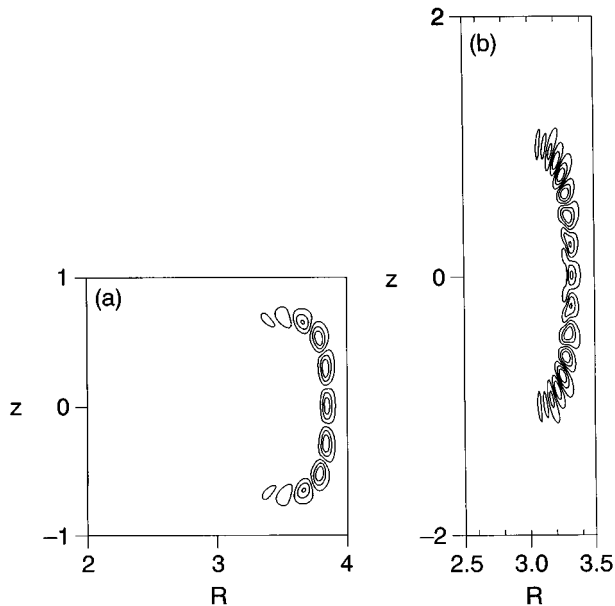


FIG. 11. Poloidal aspect ratio — $n=10$ mode structure. Level contours of the real part of the $n=10$ pressure perturbation are plotted for $A_{pol}=$ (a) 1, and (b) 4.

elongation is reduced, the mode becomes more sharply localized to the ever-increasing pressure gradient on the large major radius side of the magnetic axis. The structure of the growing $n=10$ mode is shown in Fig. 11. As the toroidal mode number increases, the modes become more localized to the equilibrium gradient.

V. EXTERNAL VERTICAL MAGNETIC FIELD

The equilibrium position of the magnetic axis along the major radius can be altered by the application of an external vertical magnetic field $B_{z,ext}$. The introduction of a uniform field pointing downward in the z -direction shifts the magnetic axis inward to smaller major radius, and creates a new magnetic separatrix on the large major radius side of the magnetic axis. An equilibrium contour plot of constant pressure in the poloidal plane for $\epsilon\beta_{pol}=10.6$ and for $B_{z,ext}=-0.06$ is shown in Fig. 12. This equilibrium is obtained dynamically like that shown in Fig. 1, with the same

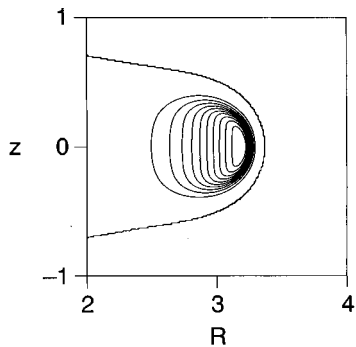


FIG. 12. External vertical magnetic field — equilibrium. Level contours of the pressure are plotted for a negative shear equilibrium with $\epsilon\beta_{pol}=10.6$ and $B_{z,ext}=-0.06$.

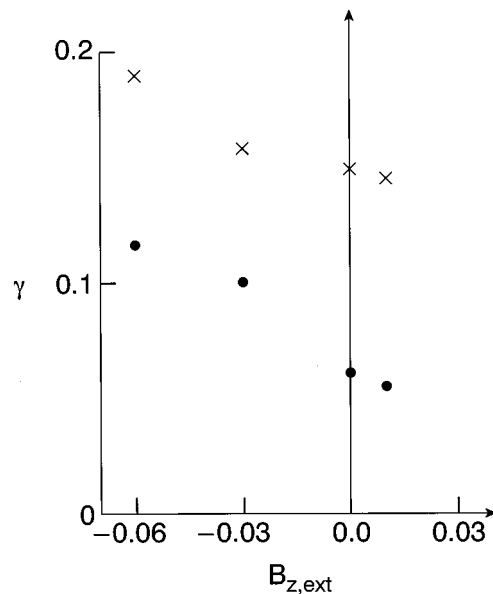


FIG. 13. External vertical magnetic field — stability. The growth rate γ , normalized to the Alfvén time, for the $n=1$ mode (circles) and the $n=10$ mode (crosses) is plotted as a function of the external vertical magnetic field $B_{z,ext}$.

initial ψ profile generating the same initial internal magnetic field, but with an additional external field $B_{z,ext}$. The pressure profile is given by the same flux function as before, $P=P_{max}g(\psi-\psi_{sep})/g(1-\psi_{sep})$, where ψ_{sep} is the value of ψ on the separatrix and $\psi_{sep}=0$ when $B_{z,ext}=0$; the pressure is zero on the open flux surfaces formed outside the new separatrix, but inside the wall. As $-(B_{z,ext})$ increases in magnitude from zero to 0.03, the position of the magnetic axis moves inward from 3.70 to 3.53. A further increase in $-(B_{z,ext})$ to 0.06 results in an additional inward shift to $R_{axis}=3.20$. The creation of a new magnetic separatrix on the large major radius side of the magnetic axis restricts the plasma to a smaller volume inside that separatrix. Since the pressure is a flux function, a comparison of the pressure surfaces in Fig. 12 for $B_{z,ext}=-0.06$ with those for $B_{z,ext}=0$ in Fig. 1(b) shows that the flux surfaces on the large major radius side of the magnetic axis are more circular in shape when $B_{z,ext}=-0.06$. Of course, the flux on the small major radius side of the magnetic axis is solely a function of R in both cases. The addition of the external vertical magnetic field alters the q -profile, but the magnetic shear around the magnetic axis is still negative and q remains above two everywhere.

The effect of an external vertical magnetic field on MHD stability is shown in Fig. 13, where the growth rate of an $n=1$ perturbation (circles) and an $n=10$ perturbation (crosses) is plotted as a function of $B_{z,ext}$. As $B_{z,ext}$ becomes increasingly negative and the magnetic axis moves inward in major radius, the growth rate of the $n=1$ mode increases, almost doubling as $-(B_{z,ext})$ increases from zero to 0.06. The growth rate of the $n=10$ mode also increases as $-(B_{z,ext})$ increases, although the increase is not as great as for the $n=1$ mode. These results demonstrate that changing the shape of the flux surfaces on the large major radius side

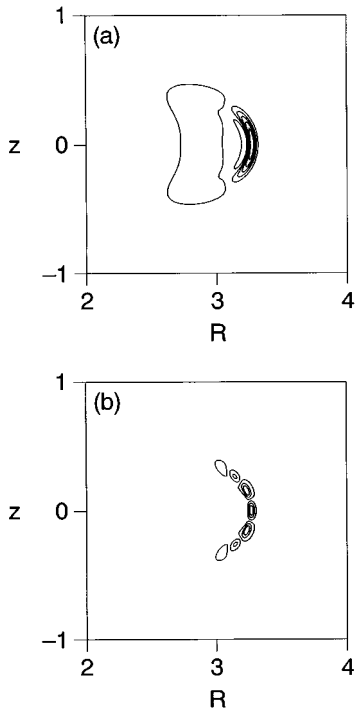


FIG. 14. External vertical magnetic field — mode structure. Level contours of the real part of the pressure perturbation in a negative shear equilibrium with $\epsilon\beta_{pol}=10.6$ and $B_{z,ext}=-0.06$ are plotted for $n =$ (a) 1, and (b) 10.

of the magnetic axis towards a more circular shape does not improve stability when $\epsilon\beta_{pol} \gg 1$. The likely cause of the increase in the growth rate is the reduced stabilizing influence of the conducting wall. Figure 14(a) is a plot of the real part of the pressure perturbation of the $n=1$ mode in the equilibrium shown in Fig. 12. A corresponding plot of the real part of the $n=10$ pressure perturbation is presented in Fig. 14(b). As the magnetic axis moves inward in major radius, away from the conducting wall at $R=R_0+a_R$, the equilibrium gradients and the modes which form on the gradients also move away from the wall. Thus, the stabilizing influence of the conducting wall is reduced. Since the $n=10$ mode is more localized in space than the $n=1$ mode, the influence of the wall on the $n=10$ mode is smaller than it is on the $n=1$ mode. When the vertical magnetic field points upward rather than downward, the magnetic axis is moved outward in major radius, closer to the conducting wall at

$R=R_0+a_R$. As $B_{z,ext}$ increases from zero to 0.01, the magnetic axis moves from $R=3.70$ outward to $R=3.74$. The stability plot in Fig. 13 shows that the growth rate of the modes decreases as the magnetic axis is moved closer to the wall.

VI. CONCLUSION

The MHD stability of high pressure tokamak equilibria with $\epsilon\beta_{pol} > 1$ is not improved by reversing the central magnetic shear and raising the safety factor q above two everywhere. At small $\epsilon\beta_{pol} \ll 1$, the equilibrium pressure is negligible and the dominant source of free energy is the gradient in the equilibrium current. Raising q above two eliminates the $q=2$ rational surface from the plasma, and with it the growing $m=2/n=1$ resistive kink (tearing) mode. However, this improvement in MHD stability does not persist as the equilibrium pressure increases and $\epsilon\beta_{pol}$ approaches unity. The physical concept of resonance at a rational magnetic surface, so important in low β tokamaks where the equilibrium current is dominant, is no longer relevant when the plasma pressure becomes much larger than the pressure in the poloidal magnetic field. Altering the current profile, and with it the q -profile, does not affect MHD stability when $\epsilon\beta_{pol}$ is no longer small.

ACKNOWLEDGMENT

This research was supported by the U.S. Department of Energy.

- ¹S.C. Cowley, P.K. Kaw, R.S. Kelley, and R.M. Kulsrud, Phys. Fluids B **3**, 2066 (1991).
- ²S.C. Cowley, Phys. Fluids B **3**, 3357 (1991).
- ³R.G. Kleva, Phys. Plasmas **3**, 2337 (1996).
- ⁴F.M. Levinton, M.C. Zarnstorff, S.H. Batha, M. Bell, R.E. Bell, R.V. Budny, C. Bush, Z. Chang, E. Fredrickson, A. Janos, J. Manickam, A. Ramsey, S.A. Sabbagh, G.L. Schmidt, E.J. Synakowski, and G. Taylor, Phys. Rev. Lett. **75**, 4417 (1995).
- ⁵E.J. Strait, L.L. Lao, M.E. Mael, B.W. Rice, T.S. Taylor, K.H. Burrell, M.S. Chu, E.A. Lazarus, T.H. Osborne, S.J. Thompson, and A.D. Turnbull, Phys. Rev. Lett. **75**, 4421 (1995).
- ⁶C. Kessel, J. Manickam, G. Rewoldt, and W.M. Tang, Phys. Rev. Lett. **72**, 1212 (1994).
- ⁷J. Manickam, M.S. Chance, S.C. Jardin, C. Kessel, D. Monticello, N. Pomphrey, A. Reiman, C. Wang, and L.E. Zakharov, Phys. Plasmas **1**, 1601 (1994).
- ⁸M.W. Phillips, M.C. Zarnstorff, J. Manickam, F.M. Levinton, and M.H. Hughes, Phys. Plasmas **3**, 1673 (1996).